ELSEVIER

Surface Science 513 (2002) 367–380

SURFACE SCIENCE

www.elsevier.com/locate/susc

Changes of local electronic structure of perfect $(VO)_2P_2O_7(1\,0\,0)$ surface in response to oxygen vacancy formation: effect of electron trapping

A. Haras [a,c,*], H.A. Duarte [b], D.R. Salahub [c], M. Witko [a]

[a] *Institute of Catalysis and Surface Chemistry, Polish Academy of Sciences, ul. Niezapominajek 9, 30-239 Kraków, Poland*
[b] *Departamento de Química—ICEx, Universidade Federal de Minas Gerais, 31.270-901 Belo Horizonte, MG, Brazil*
[c] *Steacie Institute for Molecular Sciences, National Research Council, 100 Sussex Drive, Ottawa, Ont., Canada, K1A 0R6*

Received 18 February 2002; accepted for publication 19 April 2002

Abstract

This paper reports theoretical calculations based on density functional theory applied to investigate how the formation of oxygen vacancies modify the catalytic properties of the $(VO)_2P_2O_7(1\,0\,0)$ surface. Although a detailed understanding of the structure of the perfect surface is crucial, it must be stressed that in most practical cases oxide surfaces are defective and irregular. Among the various defects occurring in the metal oxides, the oxygen vacancy at the surface has received particular attention from both experimentalists and theoreticians. In spite of its simplicity this relatively common defect has very interesting properties. In this work one type of surface oxygen monovacancy is considered—the neutral F_s^0 center i.e. vacancy with two trapped electrons. Electronic structures of vacancies at the $(VO)_2P_2O_7(1\,0\,0)$ surface are studied using a cluster model. The energetics of defect formation and the effect of electron trapping on the atomic arrangement is discussed. It is shown that the vacancies significantly modify the physical and chemical properties of the $(VO)_2P_2O_7(1\,0\,0)$ surface, thus influencing its catalytic behavior. A link between the sensitivity of the reactivity of the chemical system and the perturbation in the electronic density of the system due to the point anionic defects is demonstrated.

Keywords: Surface chemical reaction; Density functional calculations; Electron density, excitation spectra calculations; Surface defects; Surface electronic phenomena (work function, surface potential, surface states, etc.); Oxygen

1. Introduction

One of the long-term goals of surface science is to establish an understanding of the important physical properties of the surface which determine its chemical reactivity. Such knowledge could serve as a basis for the design of a surface with desired catalytic activity/selectivity. In heterogeneous catalysis, for both industrial processes and sophisticated highly controlled surface science experiments, metal oxide systems play an important role as components as well as supports in active catalytic systems. The uniqueness of metal oxides in catalytic properties appears to be associated

* Corresponding author. Address: Institute of Catalysis and Surface Chemistry, Polish Academy of Sciences, ul. Niezapominajek 9, Kraków, Poland.
E-mail address: ncharas@cyf-kr.edu.pl (A. Haras).

0039-6028/02/$ - see front matter
PII: S0039-6028(02)01781-8

with coordinatively unsaturated transition metal ions and surface defects arising from steps, corners, or vacancies [1]. Most of the chemistry at metal oxides is due to the presence of highly reactive defect sites such as cation or anion vacancies [2]. Such defects, in contrast to crystallographic shear planes, do not lead to a collapse of the lattice [3].

Complex vanadium–phosphorus oxides, which are used industrially in the synthesis of maleic anhydride (MA) from *n*-butane are of special interest to heterogeneous catalysis [4–7]. It is worthwhile to mention that the *n*-butane to MA process is the only industrially practiced process of heterogeneous selective oxidation involving alkane species. Therefore, there is a strong interest in gaining a fundamental understanding of how this system works. The selective conversion of alkanes to oxygenates has a great practical significance since alkanes are lower-cost feedstocks than their olefin counterparts and are now currently utilized [8]. On the other hand, the catalytic partial oxidation of alkanes poses a particular challenge because they are very unreactive. As a result, high temperature is generally required for C–H bond activation. Unfortunately, high temperatures also favor non-selective secondary reactions, such as combustion [9]. An effective catalyst must therefore balance the desire to achieve high conversion rates with the goal of high selectivity for partial oxidation. A fundamental understanding of how vanadium phosphorus oxide (VPO) catalysts operate would be an important source for the development of new classes of catalytic materials for alkane oxidation. It is well known that the activity of VPO catalysts appears to be associated with the presence of extended defects [10–14]. The active phase of VPO for selective *n*-butane oxidation is concluded to be vanadyl pyrophosphate, $(VO)_2P_2O_7$ [15]. Experimentally, it is observed that the surface of polycrystalline $(VO)_2P_2O_7$ presents a great variety of irregularities such as morphological defects, anion and cation vacancies, divacancies, or impurity atoms [14,16–18]. Such surface defects create sites where surrounding ions have lower coordination and, as a consequence, are more active as acidic or basic centers. Moreover, it is conjectured that the glide defects, which relieve the misfit strains between the reduced oxide surface layers and the bulk, may provide the active centers for the reaction in the form of anionic vacancies associated with the Lewis centers [10]. In addition, there is a general consensus that such surface defects play a crucial role in molecular processes at oxide surfaces [2,19]. Therefore, in order to be able to predict a defect concentration one has to determine all physical and chemical factors influencing the formation of these defects.

Theory may play at least a double role in studying defects in solids. First, the calculations may predict properties, which can be measured. Second, theory may serve also as a tool to interpret the experimental data. In many cases, developments in catalysis still depend on trial-and-error efforts, and require a great deal of intuition. A kind of 'interactive' comparison of the experimental and theoretical data is an important tool in the identification of the defect species and its electronic structure. As examples, one can mention the determination of the components of the (center) electric field gradient (EFG) around the defect, the calculation of electron paramagnetic resonance (EPR) signals, or the determination of positron annihilation characteristics [20]. A common feature of these experiments is that the measured data indirectly reflect the properties of the defect and therefore theoretical tools are needed in their interpretation. Furthermore, accurate density functional theory (DFT) calculations can supply us with information concerning the electronic state of each site, a property that is difficult to obtain directly from the experiment. In modeling, it is possible to create artificially the specific defects and to control their number and activity.

The aim of the present work is to use DFT to investigate the electronic structure of the $(VO)_2P_2O_7$ system in order to understand its catalytic properties and to rationalize the role of the oxygen vacancies. To address some of these issues we concentrate on the (1 0 0) basal plane, which is proposed to contain the active and selective sites for *n*-butane oxidation [21–23]. At the surface the F_s vacancy, which can give rise to F_s^0, F_s^+ and F_s^{2+} centers, may exist [24]. Here, the F_s^0 center corresponds to the formal removal of an O atom from the surface, whereas F_s^+ and F_s^{2+} means that one or

two electrons are removed, as well. Because of the positive charge, the F_s^+ and F_s^{2+} centers are not as good nucleophilic sites as the neutral F_s^0 centers and are not considered in this study. Since only the neutral oxygen vacancy in $(VO)_2P_2O_7$ is taken into account, F_s^0, the superscript "zero" is omitted in the following.

To model the formation of oxygen vacancies, a finite cluster model is used. Such a model reflects the local nature of the vacancy defect and mimics to some extent the real situation since the broader artifacts present in cluster calculations simulate the presence of vacancies, steps, kinks and others surface defects, which are always present in a real material. The periodic description for defects seems to be less appropriate. Although usually it is the ideal scheme for studying oxide systems in $(VO)_2P_2O_7$, the calculations would be quite expensive, due to the requirement of a large super cell following from the very low symmetry of the $(VO)_2P_2O_7$ crystal [25]. In addition, point defects break the perfect translational symmetry of the Bravais lattice and increase the complexity of the system. Furthermore, it is necessary to control the effects due to the interactions between the defect and its periodic replicas. In the periodic approach, the mutual interactions among the point defects can be strongly reduced but never completely eliminated. The model should be thus most appropriate for the simulation of rather high concentrations of defects. The understanding of the chemical and physical properties of local active defect sites of $(VO)_2P_2O_7$, allows one to answer the question of which new features are induced by defects present at the surface. Further, it may help in predicting the role of defects for the heterolytic splitting of C–H bonds in saturated hydrocarbons.

2. Crystallographic and computational details

Vanadyl pyrophosphate crystallizes within an orthorhombic layered structure with lattice constants: $a = 7.725$ Å, $b = 16.576$ Å, and $c = 9.573$ Å [25]. The active (1 0 0) plane (see Fig. 1) consists of dimeric units formed by edge-sharing two square-pyramidal VO_5 units. The apical oxygen atoms of the two groups are pointed in the opposite directions, which means that at the surface each dimeric unit has a metal–oxo group adjacent to a strong Lewis acid site, which is pointing outwards. The dimers are linked together by phosphorus atoms to form layers that, in turn, are linked together by P–O–P linkages to form the three-dimensional structure of $(VO)_2P_2O_7$. The layers are aligned so that the vanadyl groups form pairs of V═O—V═O chains pointing in the direction perpendicular to the surface. The shortest V═O protrudes always above the reduced surface.

The regular $(VO)_2P_2O_7$ surface was modeled by one layer of the bulk structure with the surface perpendicular to the (1 0 0) direction, an approximation that follows from a weak interlayer coupling [14]. The cluster chosen to represent the (1 0 0) face is in the form of $V_{10}P_6O_{50}H_{30}$, where the $V_{10}P_6O_{50}$ fragment is cut out of the (1 0 0) surface and has the geometry taken from the crystallographic data [25]. Hydrogen atoms terminate the valencies of the outer O atoms (Fig. 2). Although other embedding techniques can be more powerful, they are still in an early stage of development and in the case of transition metal oxides, clusters with hydrogen saturation (the most simple representation of the Madelung field) usually give similar results. The point-charge method, which is the most popular, often has an unfavorably strong influence on the electronic structure of the models, improving neither the stability nor the convergence properties of the cluster models. Moreover, there is still no universal prescription for determining the appropriate value of the charges and the extent of the array. Most of the essential features of a regular (1 0 0) surface of $(VO)_2P_2O_7$ are presented by the $V_{10}P_6O_{50}H_{30}$ cluster and the reliability of this approach was tested [26]. In addition, the selected cluster seems to be sufficiently large to accommodate all important chemical effects associated with the creation of the defect (removal of an oxygen ion, relaxation of nearby ions, addition of the hydrogen atoms, redistribution of the electron charge, etc.) as it includes all nearest neighbors of potential vacancies in their proper surface environment. To save computational time, calculations were performed with the geometry of the cluster frozen. The magnitude of relaxation for the defective

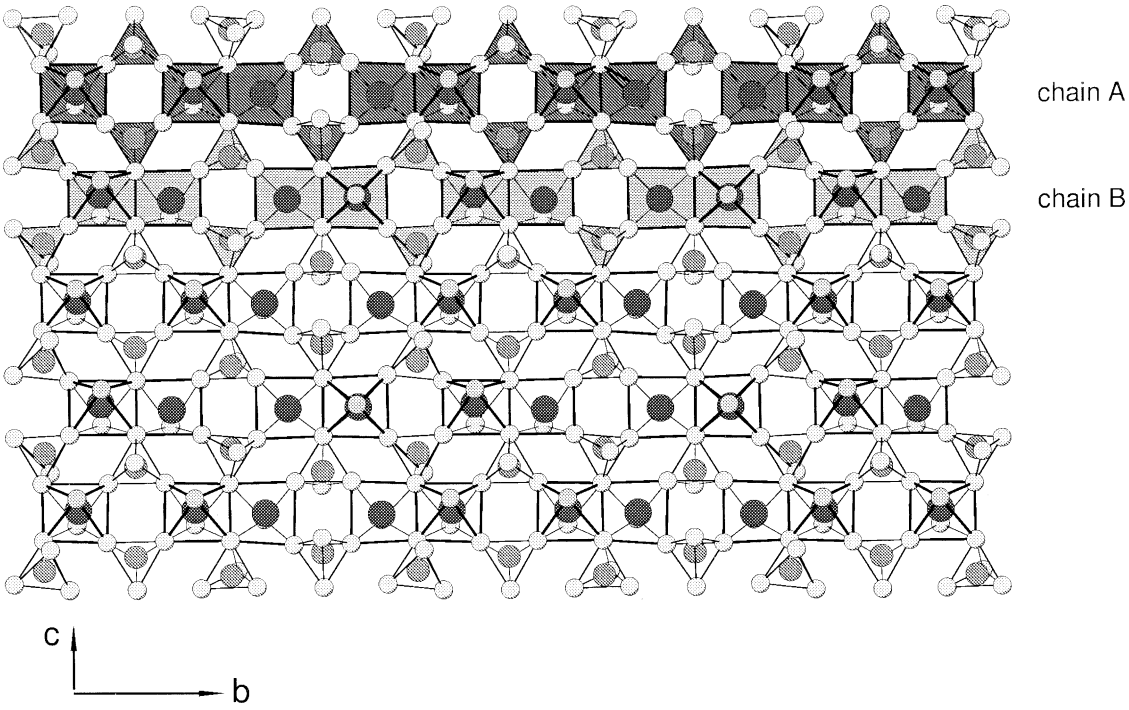

Fig. 1. Polyhedral view of the crystal structure of the reduced $(VO)_2P_2O_7(1\,0\,0)$ surface parallel to the *a*-axis. The two crystallographically inequivalent chains are shown along the *b*-axis. Throughout the paper shaded dark gray, light gray and pale gray balls represent V, P, and O atoms, respectively.

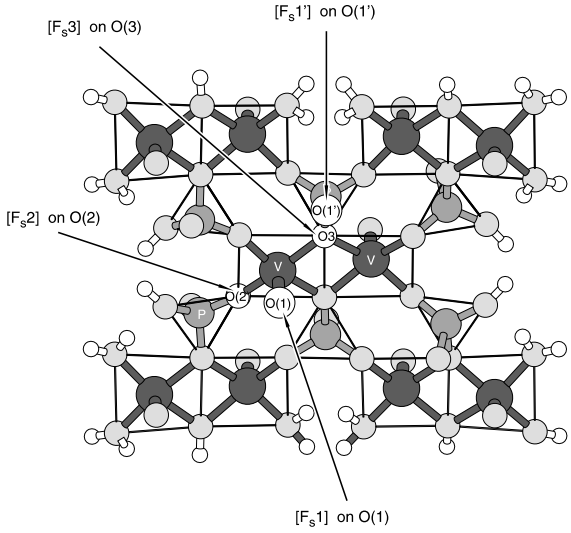

Fig. 2. Ball-and-stick model (top view) of a $V_{10}P_6O_{50}H_{30}$ cluster used to represent the $(VO)_2P_2O_7(1\,0\,0)$ surface. The labeling concerning atoms is limited to those, which are the most affected by creation of the oxygen vacancies. Arrows indicate the position of the created F_s centers at various sites in the cluster.

cluster geometries has been estimated performing additional calculations; one geometry cycle for one of the defective geometries of $(VO)_2P_2O_7$ and V_2O_5 to compare atomic forces in the vicinity of the created vacancy sites. A fact that the estimated forces for $(VO)_2P_2O_7$ have been smaller than those for V_2O_5, where the geometry relaxation did not change the trends [26], indicates the relaxation effects in vanadyl pyrophosphate being even smaller.

The calculations were carried out using DFT which is widely used in surface studies (see, for example, Ref. [27]). The linear combination of Gaussian type-orbitals-density functional Kohn–Sham (LCGTO-DF-KS) approach was applied, as implemented in the deMon suite of programs [28]. Throughout the calculation we used the Perdew-Wang-91 GGA approximation (PW91) for the exchange-correlation energy [29]. The one-electron Kohn–Sham wavefunctions for the $(VO)_2P_2O_7$ cluster were constructed using a double zeta va-

Table 1
Basis sets used in the present study [30]

Orbital basis	V	P	O	H
OBS				
DeMon	63321/531*/41+	6321/521/1*	621/41/1*	41
Conventional	15s9p5d/5s3p2d	12s8p1d/4s3p1d	9s5p1d/3s2p1d	5s/2s
ABS				
DeMon	(5,5;5,5)	(5,4;5,4)	(4,3:4,3)	(4;4)
Conventional	10s5p5d	9s4p4d	7s3p3d	4s

lence basis set (DZVP) augmented by the addition of d-symmetry polarization functions on V, P and O ions [30]. The orbital (OBS) and auxiliary (ABS) basis sets are shown in Table 1. To describe the problem of trapping electrons at the vacancy two different strategies were applied. Starting from the hypothesis that the removal of an oxygen atom leads to the formation of dangling bonds or localized V–V covalent bonds, no basis functions were placed at the position of the missing oxygen. This approach is often applied to more covalent compounds such as SiO_2 [31]. The second approach, commonly used for such ionic surfaces as MgO [32], assumes the possibility of electron localization at sites other than nuclei. Therefore the basis set of the missing atom (the so-called "ghost" atom, i.e., with zero nuclear charge) centered on the location of the missing oxygen is left to allow the transfer of electron density onto the vacant oxygen site. In addition to describing the trapped electrons the ghost atom functions are expected to improve the description of the surroundings.

Due to the high computational cost, only single point calculations were performed using the defect structures frozen at the crystal lattice positions. Thus, an idealized situation was assumed where neither relaxation nor reconstruction of the surface occurs.

3. Results and discussion

The physics of point defects in solids is very wide. Therefore, we restrict ourselves only to some specific aspects, namely to point anionic defects, which are thought to be responsible for the chemical activity of VPO-based catalysts [12]. The appropriate choice of defects may thus be an important factor for determining the acid–base behavior, catalytic activity as well as properties of the VPO surfaces. The point defects are considered on the (1 0 0) surface of $(VO)_2P_2O_7$. Although isolated oxygen vacancies do not occur under normal conditions, they may serve as a first step in the formation of more realistic defect structures. The stability of the defects at the different sites is compared and the consequence of the results for the activity of the material is discussed. Next, the similarities and differences between our defect model and a perfect non-defective cluster are highlighted. Since it is of special interest to understand how the spatial arrangement of the vacancy reflects the high anisotropy of the material, we focus on the modifications of the degree of covalency of the V–O and P–O bonds as a function of the different environments and on the localization of the excess charges.

3.1. Energetics of defects

The relative thermodynamic stability of the various sites where F_s centers can be formed at the $(1\,0\,0)(VO)_2P_2O_7$ surface is directly connected with the energy required to remove an oxygen species from the surface. Generally, the process of F_s^{n+} defect $(n = 0, 1, 2)$ formation at the surface can be represented by the following formal reaction:

$$S([(VO)_2P_2O_7]) \rightarrow S([(VO)_2P_2O_7]F_s)^{n+} + O^{n-}$$

with terms referring to the unperturbed system $S([(VO)_2P_2O_7])$, the system with the defect $S([(VO)_2P_2O_7]F_s)^{n+}$ and the extracted atomic species O^{n-} together with the number of electrons

removed from the crystal. Therefore the difference between the total energy of the system with the vacancy $E([(VO)_2P_2O_7]F_s)$ and the energy of the free oxygen species $E(O^{n-})$ and the total energy of the vacancy-free system $E([(VO)_2P_2O_7])$, can be used to calculate the neutral vacancy-formation energy

$$E_f(F_s) = E([(VO)_2P_2O_7]F_s)^{n+} + E(O^{n-}) - E([(VO)_2P_2O_7]).$$

The reference in this case is assumed to be the vacuum and the two species are assumed to be infinitely far apart when separated. For this type of oxygen vacancy, four possible defect sites are considered (Fig. 2): vanadyl on-top oxygen O(1) coordinated to one vanadium F_s1, on-top phosphorus oxygen O(1′) singly coordinated to one phosphorus F_s1', bridging oxygen O(2) doubly coordinated to one phosphorus F_s2 and the oxygen O(3) triply coordinated to one phosphorus and two vanadium planar F_s3, respectively. Each of these defects has a different coordination number that results from the different number of broken bonds and, in addition, each of them has a different arrangement. The formation energies of such defects may serve as indicators to determine their concentration.

As far as the authors are aware, there is no experimental determination of the energy needed for oxygen vacancy formation in the case of the $(VO)_2P_2O_7(1\,0\,0)$ surface. Table 2 gives a comparison of DFT results for the oxygen removal energies with the previous theoretical calculations which used the crystallo-chemical model of active sites (CMAS) introduced by Ziółkowski [33–36]. This model is based on the bond-strength-coordination number relation, first formulated by Pauling. According to the CMAS model, the oxygen atoms in particular positions at the surface are characterized by calculating the sum of Pauling's bond strengths. Since our data showed that to predict the energetics of the defects no ghost function at the vacancy center is needed, we report only the results carried out for defects without basis functions at the center of the vacancy.

Table 2 indicates that the oxygen vacancy energy, as a function of defect location, decreases steadily as the coordination of the oxygen site is reduced and points to the formation of vacancies in the axial rather than in equatorial position as more favorable. The energy is reduced from 8.02 eV for defects created on high-coordinated surface sites to 6.34 eV for defects on low-coordinated oxygen atoms. The energetic cost of removing the oxygen doubly coordinated to one phosphorus and to one vanadium center is smaller by 1 eV in comparison to the triply coordinated F_s. Further, reduction of the energetic cost occurs when the F_s centers are formed at the singly oxygen atom coordinated to one vanadium, and the removal energy decreases by 0.26 eV more when we pass to the oxygen singly coordinated to the phosphorus site. Overall, the difference in vacancy formation energy between the low- and high-coordinated defect centers in the unrelaxed configuration is 1.64 eV. This quite large value indicates that low-coordinated F_s centers are easier to form, and hence thermodynamically preferred. The influence of the vacancy-centered basis function (see Table 2, numbers in parenthesis), is negligible.

Let us now compare our results with those obtained using the aforementioned CMAS model.

Table 2
DFT vs. CMAS defect formation energies, E_f, for the F_s neutral oxygen vacancies at the $(VO)_2P_2O_7(1\,0\,0)$ surface, evaluated as discussed in the text, eV

Method	Vacant			
	O(3) in-plane [F_s3]	O(2) in-plane [F_s2]	O(1) terminal [F_s1]	O(1′) terminal [F_s1']
DFT	8.02 [7.94][a]	7.04 [7.01][a]	6.56 [6.51][a]	6.34 [6.30][a]
CMAS[b]	8.39	7.87	5.06	3.92
Diff. (%)	4.4	10.6	22.9	38.2

[a] In parentheses the values of E_f with the inclusion of vacancy-centered basis functions.
[b] The CMAS results are taken from Ref. [34].

The energy of the formation of $[F_s(1')]$ neutral vacancy involving P=O bonding is 6.34 eV, about 1.6 times larger than estimated by using the CMAS, which yields an energy of 3.92 eV for such a defect. The agreement between the two approaches is clearly better in the case of the oxygen vacancy $[F_s(1)]$ created on the terminal O(1) site where the difference is 1.5 eV. On passing from low- to high-coordinated anionic defects the variations between the values of the vacancy formation energy obtained using both theoretical methods become significantly smaller. The energetic cost of the $[F_s(2)]$ defect connected with the removal of an O atom from the bridging V–O–P site is 7.04 eV and compares quite well with 7.87 eV, the value deduced from CMAS. The error between these two methods is only about 10%. We note that while we are going from doubly to triply coordinated defects $[F_s(3)]$ the variation of the value of their energy formation even decreases (the estimated error about 4%). Although both approaches give somewhat different values for the formation of vacancies, they both agree that the neutral F_s centers should be preferentially formed at low coordination sites. Further, they predict the same order of energies needed to create the vacancies. This is particularly important since they assume completely different theoretical schemes for evaluating the energetics. Experience with the other theoretical estimates of vacancy formation energy clearly showed that they may differ even by an order of magnitude from method to method [37,38]. Therefore, our purpose is to discuss and understand trends rather than to produce numerical results of high accuracy. Experimental studies are thus awaited to confirm our predictions, although it should be mentioned that the comparison with experimental measurements must always be made with caution due to approximations made in the modeling.

The foregoing analysis of the neutral oxygen vacancy at the (1 0 0) surface of $(VO)_2P_2O_7$ leads to the conclusions that the formation of the low-coordinated centers such as O(1) and O(1′) is energetically less costly than for high-coordinated centers and may reflect the requirement of such centers in the oxidation of *n*-butane to maleic anhydride over VPO catalysts [39].

3.2. Electronic structure of unperturbed and defective (1 0 0) $(VO)_2P_2O_7$ surfaces

3.2.1. The perfect (1 0 0) $(VO)_2P_2O_7$ surface

Since it is well-known that a question concerning F_s centers is related to the electronic structure, the discussion would be incomplete without a more detailed analysis of the charge distribution of these sites, which in addition should help in understanding the properties of $(VO)_2P_2O_7$ as a catalyst. Prior to discussing the defective surface and the nature of the active sites, the structure of the non-defective, perfect (1 0 0) surface of $(VO)_2P_2O_7$ has to be analyzed. It is well-known that depending on the oxidation state of the metal ion and on its environment (coordination structure), the metal–oxygen bonds may be more or less polarized and therefore the oxygen ion may or may not exhibit nucleophilic properties. The degree of ionicity is of fundamental importance and has direct consequences on the reactivity of chemisorbed species in the preliminary steps of the catalytic process. One measure of the ionicity of a bond is the Löwdin population analysis. As we have applied two different strategies for describing electrons trapped at the anion vacancy, without and with vacancy-centered basis functions, the Löwdin analysis seems to be better suited than the more widely used Mulliken scheme. Attempts to identify the degree of electron localization with Mulliken population analysis may lead to frustrating results (see for example Ref. [40]) because, depending on the basis set used, the results oscillate from almost full localization in the vacancy to complete delocalization over neighboring ions. In contrast, the Löwdin populations are suggested to be less sensitive to basis set changes [41].

In Table 3 we list Löwdin charges of selected atoms for the $V_{10}P_6O_{50}H_{30}$ cluster modeling the defect-free $(VO)_2P_2O_7$(1 0 0) surface. The population analysis shows that the vanadium and phosphorus atoms are always positive with atomic charges of about 0.4 a.u. for V and 1.2 a.u. for P at the center of the cluster. The terminal oxygen O(1′) coordinated to one phosphorus carries the highest negative charge (−0.61 a.u.) and is followed by both high-coordinated oxygen atoms O(3) and O(2), (−0.46, and −0.43 a.u., respectively) and

Table 3
Löwdin charges and Mayer bond indices of various V–O and P–O bonds of unrelaxed defect-free $(VO)_2P_2O_7(1\,0\,0)$ surface[a]

Charges q, bond orders p	a.u.
q(V)	0.45
q(P)	1.21
q(O(1))	−0.19
q(O(1′))	−0.61
q(O(2))	−0.43
q(O(3))	−0.46
p(O(1))	2.32
p(O(1′))	1.74
p(V–O(2)–P)	0.50/1.33
p(V–O(3)–V)	0.38/0.40
P	0.89

[a] Positions of selected atoms in model cluster are indicated in Fig. 2.

vanadyl oxygen O(1) (−0.19 a.u.). Thus, the results indicate that oxygen atoms with different coordination numbers behave like different chemical species. In particular, the Coulomb field created by only one nearest V in the O(1) position is not strong enough to stabilize an O ion with the formal charge of −2 leading to the particularly low value of the net charge on O(1) species. The increased charge at the higher-coordinated oxygen sites hints at their increased local reactivity with respect to nucleophilic attacks. Further, the actual ionic charges differ greatly from their nominal values, reflecting significant covalency of V–O interatomic binding, as suggested by basic chemical intuition and previous Mulliken results for that system [26]. Taking the Mayer bond order [42,43] as a measure of the covalent properties of V–O bonds, one can conclude that the bonds between vanadium centers and terminal oxygen exhibit more covalent than ionic bonding character, whereas in the case of bridging oxygens the situation is reversed.

3.3. The surface F_s^0 center

Generally, formation of a neutral F_s center (see Fig. 2) corresponds to removal of an oxygen atom from the regular surface and the two electrons associated with the formal O^{2-} dianion being left behind due to electrostatic stabilization by the Madelung potential of the crystal. Such two electrons are less strongly bound than the electrons of an O^{2-} ion on the $(VO)_2P_2O_7$ surface and their presence makes the surface electronically neutral. Owing to a considerable reduction of the Pauli repulsion by F_s compared with an O^{2-} center, one may expect that in case of such a center the adsorbates will be able to approach the (1 0 0) surface of $(VO)_2P_2O_7$ more closely. The trapped electrons can either be localized in the center of the vacancy or delocalized over the ions around the cavity. The effect of the creation of such a vacancy on the electronic distribution is studied through the Löwdin distribution. Electron transfer, defined as the difference in Löwdin charge between atoms in the defective surface and atoms in equivalent positions on the clean surface, is tabulated in Tables 4 and 5 and illustrated in Figs. 3 and 4 for the case without and with vacancy-centered basis functions. Both tables contain only the values of electron transfer grater than $0.01e$, as we think it is more useful to put small changes (<0.01 a.u.) upon creation of F_s centers on the figures. Therefore, Figs. 3 and 4 contain all changes >0.01 a.u., thus give a nice visual picture of the distorted electron density and

Table 4
The charge difference >0.01 a.u. with respect to the clean surface ($\Delta = q - q_{clean}|e|$) computed using the Löwdin scheme for the $V_{10}P_6O_{50}H_{30}$ clusters with neutral oxygen vacancies without including the ghost orbital[a]

Vacant	ΔV	ΔV	ΔP	ΔP	$\sum_{negative}$	$\sum_{positive}$	$\sum_{total}$	$\sum_t -q$[b]
[F_s3] O(3)	−0.14	−0.15	−0.11	0.00	−0.49	0.02	−0.46	−0.01
[F_s2] O(2)	−0.16	−0.01	0.00	−0.20	−0.44	0.02	−0.42	0.01
[F_s1] O(1)	0.01	−0.02	0.00	−0.01	−0.11	0.02	−0.09	0.10
[F_s1′] O(1′)	−0.03	−0.03	−0.17	0.00	−0.45	0.01	−0.44	0.17

A positive or negative sign means an increase of electrophilicity or nucleophilicity of the surface centres, respectively.
[a] Atom labels refer to Fig. 2.
[b] The difference between the total sum of negative and positive contributions from affected atoms and effective charges assigned to O^{2-} missing lattice ion. Positive values indicate charge distributed away from the surface plane.

Table 5
The charge difference >0.01 a.u. with respect to the clean surface ($\Delta = q - q_{\text{clean}}|e|$) computed using the Löwdin scheme for the $V_{10}P_6O_{50}H_{30}$ clusters with neutral oxygen vacancies including the ghost orbital at their centres[a]

Vacant	ΔV	ΔP	ΔP	ΔO(3)	ΔO(2)	ΔO(1)V	ΔO(1)P	$\sum_{\text{negative}}$	$\sum_{\text{positive}}$	$\sum_{\text{total}}$	$\sum_{\text{t}}+G$[b]
$[F_s3]$ O(3)	−0.01	0.18	0.00	$-0.17G$[c]	0.00	−0.01	0.03	−0.06	0.23	0.17	0.00
$[F_s2]$ O(2)	0.01	0.00	0.19	0.01	$-0.20G$[c]	0.01	0.00	−0.03	0.24	0.21	0.01
$[F_s1]$ O(1)	0.20	0.00	−0.01	0.00	0.00	$-0.03G$[c]	−0.01	−0.11	0.20	0.09	0.06
$[F_s1']$ O(1′)	−0.02	0.17	0.00	0.00	0.00	−0.03	$0.18G$[c]	−0.22	0.18	−0.04	0.14

A positive or negative sign means an increase of electrophilicity or nucleophilicity of the surface centres, respectively.

[a] Atom labels refer to Fig. 2.

[b] The sum of the total positive and negative contributions and the contributions from the Ghost atom. Positive values indicate charge distributed away from the surface plane.

[c] G—means the changes of an electron density on the ghost atom centered in vacancy site. A negative sign means and excess of electron density as compared to a missing O atom.

indicate how the electrons left behind after removal of the respective oxygens are distributed among the remaining atoms. The last four columns in Tables 3 and 4 list all changes caused by the created defects. The first of them contains the sum of the electron gains on atoms; the second is the sum of the electron loss on atoms, and the third one is the sum of the previous two. The last column is the sum of the third column and the effective charge of the removed oxygen atom in the case of no basis sets in the vacancy center and the amount of charge that resides at the orbitals centered at the vacancy site in case when the ghost atom is included. When we look at the values of effective charge variations on ions in the case with no orbital basis at the cavity (Table 4, Fig. 3) we can see that the whole charge assigned to the O^{2-} lattice ion, which before occupied the same position, is distributed on nearest-neighbor ions. Thus, as a consequence of this process, the trapped electrons are finally ejected from the vacancy and have considerable weight on the nearest and even next-nearest oxygen ions or are extended toward the vacuum region. On the contrary, the presence of basis sets in the cavity helps in accumulating the charge.

When an O atom is removed from the perfect cluster in position $[F_s3]$ three bonds to the neighboring atoms are broken and the resulting dangling bonds hybridize. This leads to an alteration in the electronic structure at sites neighboring the defect by changing the charge on the ions. The creation of this vacancy induces the strongest variation with the decrease of the positive charge of the V and P atoms situated in the central part of the cluster. In effect, the creation of such vacancies renders them less electrophilic. It can be seen that two vanadium and one phosphorus are about 0.14, 015 and $0.11|e|$ less positively charged than they are in the perfect surface model. The charge on other ions (see Fig. 3) differ from that of the clean surface by no more than $0.03|e|$ and are marked as small balls on the figure. When the ghost orbital was included in the $[F_s3]$ type vacancy, its population amounts to $0.63|e|$. This is more than in the perfect crystal lattice ($-0.46|e|$) (see Table 5) and the excess of negative charge ($0.17|e|$) (see Fig. 4, Table 5) is attracted mainly from the P atom in the vicinity of the vacancy center. In this sense, an $[F_s3]$ center resembles to some extent the regular missing O^{2-} lattice site of $(VO)_2P_2O_7$. The compensating charge is uniformly spread over the atoms in the first shell around the vacancy whereas the distribution of charges on the other atoms of the cluster remains nearly unchanged.

The situation is similar when the defect is created in an $[F_s2]$ position that corresponds to an O vacancy located in the V–O–P bridge. If we neglect the ghost orbitals, the creation of the $[F_s2]$ vacancy induces the strongest variation with the decrease of the positive charge of the V and P atoms situated in the central part of the cluster. This is demonstrated in Table 4 and in a graphical way in Fig. 3. One can see that there is roughly $0.16e$ on the nearest (central) vanadium atom and $0.20e$ on the nearest phosphorus atom. The rest of the charge

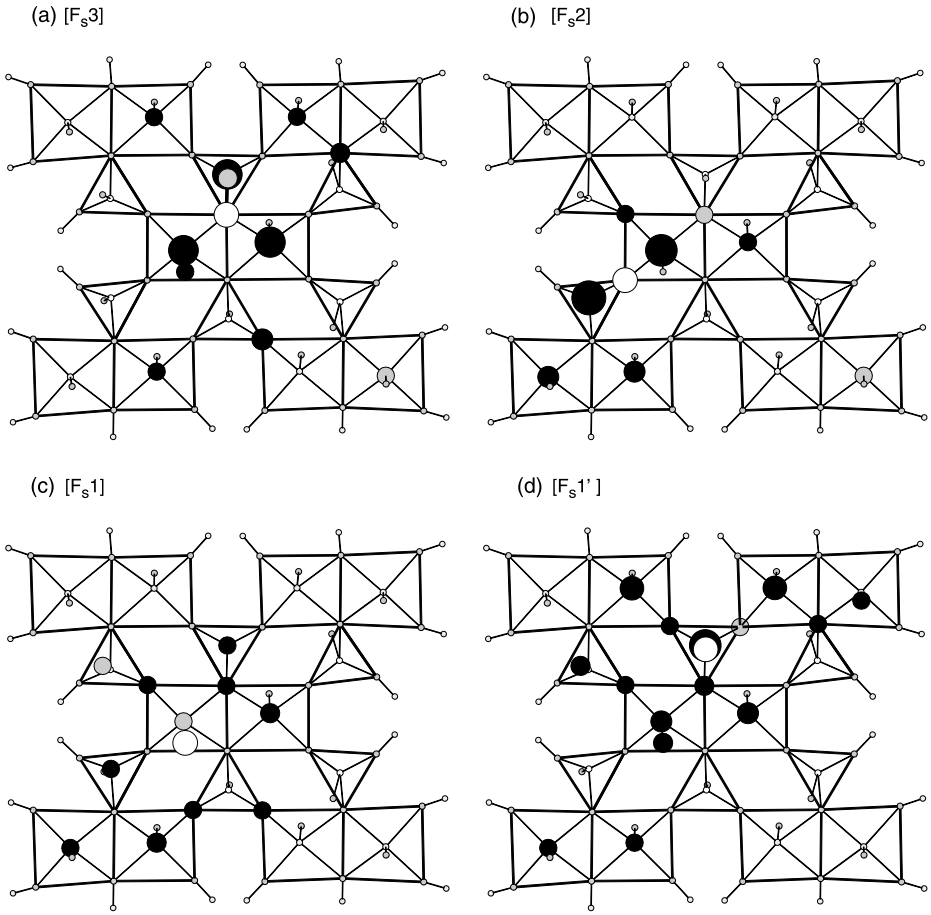

Fig. 3. Reorganization of the electron charge upon creation of different defect sites without inclusion of ghost orbitals. The oxygen vacancy is positioned on: (a) triply coordinated oxygen; (b) doubly coordinated oxygen; (c) vanadyl oxygen; (d) terminal phosphorus oxygen and are represented by open balls. The electron gain and loss on the atoms is depicted by dark and light gray spheres, respectively. The values of charge transfer, measured by Δ defined in Table 4, are reflected by different sizes of the balls. The gross (above 0.1 a.u., see Table 4 for values designation) and the small (about 0.01 a.u.) changes are represented by large and small circles, respectively. All further points in these pictures correspond to unaffected atoms.

left behind after removal of the oxygen is distributed in a more distant region. Thus, only one V atom on the central part loses electrophilic character whereas the second remains almost unchanged. If the ghost orbital is included in the V–O–P vacancy, we observe a different effect: the P center becomes more positively charged with respect to the perfect cluster (see Fig. 4, Table 5). The screening charge on the vacancy is almost restricted to the vacancy and its nearest-neighbors. The charge on the vacancy $[F_s2]$ is $0.64|e|$; which is $0.2|e|$ greater than in the perfect cluster. Again, as it was in the previous vacant center, the excess charge accumulated at the $[F_s2]$ vacancy follows from neighboring P atoms. Similarly to the vacancy formed on triply coordinated O, the $[F_s2]$ type vacancy does not change the strength of the acidic character of the V center.

The generation of a low-coordinated vacancy on the $(VO)_2P_2O_7(1\,0\,0)$ surface by removal of terminal oxygens leads to the creation of one dangling bond at the neighboring atom. Here we have two possibilities: a vacancy created by removing an oxygen that is singly coordinated to one vanadium

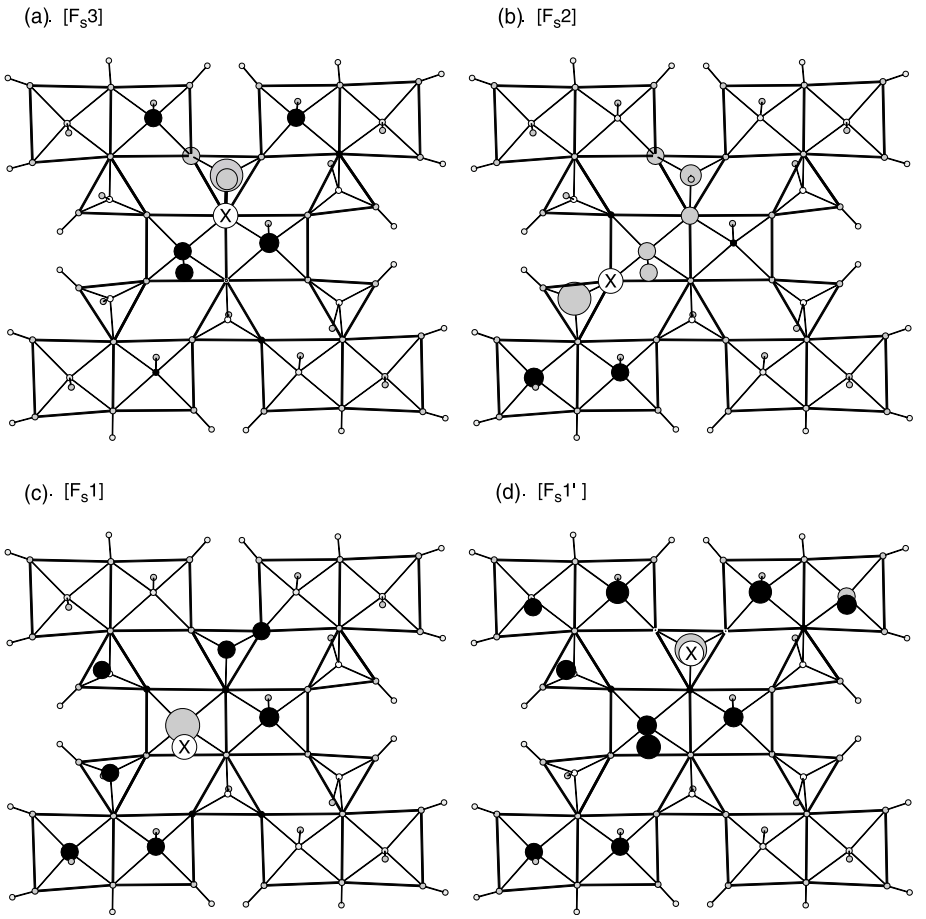

Fig. 4. Reorganization of the electron charge upon creation of different defect sites with inclusion of ghost orbitals. The oxygen vacancy is positioned on: (a) triply coordinated oxygen; (b) doubly coordinated oxygen; (c) vanadyl oxygen; (d) terminal phosphorus oxygen and are represented by open balls and marked with X letter to point out the presence of ghost atom. The electron gain and loss on the atoms is depicted by dark and light gray spheres, respectively. The values of charge transfer, measured by Δ defined in Table 5, are reflected by different sizes of the balls. The gross (above 0.1 a.u., see Table 5 for values designation) and the small (about 0.01 a.u.) changes are represented by large and small circles, respectively. All further points in these pictures correspond to unaffected atoms.

or an oxygen bonded to one phosphorus atom. Let us first consider the vacancy formed by removal of a vanadyl oxygen atom. When we neglect the ghost orbital the trapping electrons are more diffuse than in the case of high-coordinated vacancies and are shared almost equally by the nearest and even next nearest neighbors (see Fig. 3, Table 4). Inclusion of ghost orbitals results in the increase of the positive charge (oxidation) of the V center, which is only partially $(0.11|e|)$ (Fig. 4, Table 5) compensated by the decrease of the charge of lattice ions in its neighborhood. The resulting growth of the electrophilic character of the unsaturated vanadium atoms makes them suitable sites for catalytic processes, especially for very demanding oxidation of saturated hydrocarbons. It is in agreement with the observation that an acid surface is necessary to facilitate desorption of an acid product such as MA from the surface to avoid deeper oxidation. One may also notice that the created $[F_s1]$ center is not electron deficient $(-0.22 = -0.19 - 0.03)$ and, according to our calculations,

does not want to accept further electrons. The fact that the atoms located at the other sites of the cluster remain almost unchanged means that the electrons of the V atom in the vicinity of the vacant center ($0.20|e|$) are mainly extended above the surface. The formation of the second type of low-coordinated vacancy center [F_s1'], created above a phosphorus atom, results in the reduction of P (see Table 4 and Fig. 3). The missing electrons are distributed among the first and second neighbors and part of them go above the surface ($0.17|e|$). The inclusion of the ghost orbitals gives a completely different physical picture (see Table 5, Fig. 4). Due to the more ionic character of P=O bonding with respect to a V=O bond, $0.18|e|$ left the vacancy, in which $0.14|e|$ is extended above the surface. The 0.2 electrons arriving from the P atom have considerable weight on almost the whole cluster.

The results obtained with ghost functions clearly point out that two electrons trapped in equatorial surface oxygen vacancies interact much more strongly with their nearest-neighboring atoms than the vacancy created in the plane above the surface. Furthermore, for high-coordinated F_s centers a substantial ability to attract electron density from their nearest-neighbors is observed; the [F_s2] and [F_s3] vacancies accumulate 0.17 and $0.20|e|$ (see Table 5) more than was associated with the missing oxygens atoms. The [F_s1] vacancy accumulates the same charge as was associated with the missing oxygen atom whereas [F_s1'] behaves completely different by transferring 0.18 electrons to above the plane. The maximum electron density in the cavity ($0.20e$) created at the $(VO)_2P_2O_7$(1 0 0) surface is found in the case of the vacancy created on the oxygen sites linking corner-sharing phosphorus tetrahedra and vanadyl octahedra (V–O–P) in the active plane. A redistribution of electron charge accompanying high-coordinated vacancy formation happens exclusively within the surface plane, whereas in the case of low-coordinated vacant centers [F_s1] and [F_s1'] one can observe that part of the charge (0.06, 0.14, respectively) moves from the site of the perturbation toward the vacuum. Both highly coordinated vacancies do not change the strength of acidity of unsaturated V centers and may be precursors for the formation of more extended glide shear planar defects (see high-resolution and in situ electron microscopy studies reported by Gai and Kourtakis [12]). The vacancy formed above V enhances the acidity of one V from the V–V pair, which seems to be necessary to facilitate the desorption of an acid product such as maleic anhydride from the surface to avoid deeper oxidation [44]. The close agreement between experiment and the present theoretical findings as to the role of oxygen vacancies in $(VO)_2P_2O_7$ supports the necessity of including the orbital basis function at the vacancy center for the proper description of the effects induced by point defects and for understanding certain aspects of the experimental observations.

4. Conclusions

The results of our calculations support the necessity of including the orbital basis function at the vacancy center for the proper description of the effects induced by point defects in order to understand certain aspects of the experimental observations and may be summarized as follows:

- the anion vacancies are preferentially situated on low-coordinated sites;
- the presence of isolated oxygen vacancies only moderately affects the electronic structure; the electronic modifications are mostly localized on the first neighbors;
- two electrons trapped in equatorial surface oxygen vacancies interact more strongly with their nearest neighbors than the vacancies created in the axial plane e.g. above the surface, where electrons are more diffuse;
- different oxygen vacancies at the $(VO)_2P_2O_7$-(1 0 0) surface will have different chemical reactivity toward adsorbed molecules; the singly coordinated vacancy created at the vanadyl oxygen enhances the acidic character of the vanadium atoms, which is necessary to facilitate the desorption of an acidic product such as maleic anhydride from the surface to avoid deeper oxidation;
- the high-coordinated vacancies (in particular V–O–P) do not influence the acidity of V but

form high electron density regions suitable for nucleophilic attacks.

Although the surface defect modeling used here is simplified, it offers a good insight into the real physical phenomena, especially when the concentration of defects is relatively small. The global analysis of the results agrees with the experimental data and the physical concept of the performance of VPO as catalysts. We are aware of the fact that interactions between the two isolated vacancies might modify their formation energies, and it is desirable that this question should be addressed by explicit calculations in future work.

Acknowledgements

Financial support from the State Committee for Scientific Research in Poland for support of this work (Grant No. 3T09A 07719) and the Brazilian Agency FAPEMIG are acknowledged. Some of the authors (H.A.D. and A.H.) would like to thank the members of the Steacie Institute for Molecular Sciences (NRC, Ottawa) for their hospitality during the course of this work and for computer time.

References

[1] M.A. Barteau, Chem. Rev. 96 (1996) 1413.
[2] P.J. Gellings, H.J.M. Bouwmeester, Catal. Today 58 (2000) 1.
[3] B. Grzybowska-Świerkosz, Appl. Catal. A 157 (1999) 409.
[4] W.H. Cheng, Appl. Catal. A 147 (1996) 55.
[5] Y. Schuurman, J.T. Gleaves, Catal. Today 33 (1997) 25.
[6] T. Shimoda, T. Okuhara, M. Misono, Bull. Chem. Soc. Jpn. 58 (1985) 2163.
[7] A. Brückner, B. Kubias, B. Lücke, Catal. Today 32 (1996) 215.
[8] K. Shima, M. Hatano, Appl. Surf. Sci. 121/122 (1997) 452.
[9] F. Cavani, F. Trifirò, Appl. Catal. A 157 (1997) 195.
[10] P.L. Gai, Acta Cryst. B 53 (1997) 346.
[11] Z. Hiroi, M. Azuma, Y. Fujishiro, T. Saito, M. Takano, F. Izumi, T. Kamiyama, T. Ikeda, J. Solid State Chem. 146 (1999) 369.
[12] P.L. Gai, K. Kourtakis, Science 267 (1995) 661.
[13] A. Satsuma, Y. Tanaka, T. Hattori, Y. Murakami, Appl. Surf. Sci. 121/122 (1997) 496.
[14] P.T. Nguyen, A.W. Sleiht, N. Roberts, W.W. Warren, J. Solid State Chem. 122 (1996) 259.
[15] V.V. Guliants, J.B. Benziger, S. Sundaresan, N. Yao, I.E. Wachs, Catal. Lett. 32 (1995) 379.
[16] F. Richter, H. Papp, Th. Götze, G.U. Wolf, B. Kubias, Surf. Interface Anal. 26 (1998) 736.
[17] N. Duvauchelle, E. Bordes, Catal. Lett. 57 (1999) 81.
[18] V.A. Zazihigalov, J. Haber, J. Stoch, I.V. Bacherikova, G.A. Komashko, A.I. Pyatnitskaya, Appl. Catal. A 134 (1996) 225.
[19] V.E. Henrich, P.A. Cox, The Surface Sciences of Metal Oxides, Cambridge University Press, Cambridge, 1994.
[20] M.J. Puska, S. Pöykkö, M. Pesola, R.M. Nieminen, Phys. Rev. B 58 (1998) 1318.
[21] F. Cavani, S. Ligi, T. Monti, F. Pierelli, F. Trifirò, S. Albonetti, G. Mazzoni, Catal. Today 61 (2000) 203.
[22] V.V. Guliants, J.B. Benziger, S. Sundaresan, I.E. Wachs, J.-M. Jehng, Catal. Today 28 (1996) 275.
[23] G. Koyano, T. Okuhara, M. Misono, Catal. Lett. 32 (1995) 205.
[24] E. Scorza, U. Birkenheuer, C. Pisani, J. Chem. Phys. 107 (1997) 9645.
[25] Yu. E. Gorbunova, S.A. Linde, Sov. Phys. Dokl. 24 (1979) 138.
[26] M. Witko, R. Tokarz, J. Haber, K. Hermann, J. Mol. Catal. A 166 (2001) 59.
[27] M.J. Gillan, L.N. Kantorovich, P.J.D. Lindan, Curr. Opin. Solid State Mater. Sci. 1 (1996) 820.
[28] The DFT-LCGTO program package deMon was developed by A. St.-Amant and D.R. Salahub (University of Montreal). Here a modified version deMon-KS4p2 with extensions by L.G.M. Pettersson and K. Hermann is used. To calculate the first order post SCF properties in combination with deMon-KS4p2 the program deMon-Prop3p0 is applied. (www.sao.nrc.ca/sims/deMon).
[29] K. Burke, J.P. Perdew, M. Levy, in: J.M. Seminario, P. Politzer (Eds.), Modern Density Functional Theory: A Tool for Chemistry, Theoretical and Computational Chemistry, vol. 2, Elsevier, Amsterdam, 1995.
[30] N. Godbout, D.R. Salahub, J. Andzelm, E. Wimmer, Can. J. Phys. 70 (1992) 560.
[31] G. Pacchioni, Solid State Sci. 2 (2000) 161.
[32] Y.F. Zhukovskii, E.A. Kotomin, P.W.M. Jacobs, A.M. Stoneham, J.H. Harding, J. Phys.: Condens. Matter 12 (2000) 55.
[33] J. Ziółkowski, E. Bordes, P. Courtine, J. Catal. 122 (1990) 126.
[34] J. Ziółkowski, E. Bordes, P. Cortine, in: G. Centi, F. Trifiró (Eds.), New Developments in Selective Oxidation, Elsevier Science Publishers, Amsterdam, The Netherlands, 1990, p. 625.
[35] J. Ziółkowski, E. Bordes, P. Courtine, J. Mol. Catal. 84 (1993) 307.
[36] J. Ziółkowski, J. Catal. 100 (1986) 45.
[37] C. Sousa, J. Casanovas, J. Rubio, F. Ilias, J. Comp. Chem. 14 (1993) 680.

[38] G. Pacchioni, A.M. Ferrari, A.M. Marquez, F. Ilias, J. Comp. Chem. 18 (1996) 617.
[39] J.B. Benziger, V. Guliants, S. Sundaresan, Catal. Today 33 (1997) 49.
[40] A.M. Ferrari, G. Pacchioni, J. Phys. Chem. 99 (1995) 17010.
[41] K.B. Lipkowitz, D.B. Boyd, in: Reviews in Computational Chemistry, vol. 5, VCH Publishers, 1994.
[42] I. Mayer, Chem. Phys. Lett. 97 (1983) 270.
[43] I. Mayer, J. Mol. Struct. (Theochem) 149 (1987) 81.
[44] J.C. Védrine, Topics in Catal. 11/12 (2000) 147.